CHEMPHYSCHEM

DOI: 10.1002/cphc.201100680

Lipid Diffusion within Black Lipid Membranes Measured with Dual-Focus Fluorescence Correlation Spectroscopy

Kerstin Weiß and Jörg Enderlein*[a]

We present an overview of the application of dual-focus fluorescence correlation spectroscopy (2f-FCS) for the measurement of diffusion coefficients within free-standing lipid membranes. The first part gives a detailed theoretical analysis of the expected performance of 2f-FCS, in particular about the sensitivity of the method with regard to precise focus position and to aberrations caused by refractive index mismatch or cover slide thickness deviation. After describing the experimental details of the 2f-FCS setup and the preparation of free-standing black lipid membranes (BLMs), we apply the method to study the diffusion of lipids within BLMs as a function of lipid composition and of ion valency and ionic strength of the surrounding buffer.

1. Introduction

Molecular diffusion is of fundamental importance for all biological systems as it constitutes one of the basic transport mechanisms of molecules within and between cells. A particular type of diffusion is the translational diffusion of molecules within lipid bilayers such as cell membranes. There, the speed of diffusion determines how fast different membrane proteins can interact after, for example, ligand binding and activation. Thus, investigating the diffusion in membranes can yield important information for the understanding of function and interaction of trans-membrane and membrane-associated molecules.

Biological membranes consist of a lipid bilayer made up of phospho- and sphingolipids as well as cholesterol. Moreover, proteins are either incorporated into the bilayer (integral membrane proteins) or externally bound to it (peripheral membrane proteins). Due to their complexity, quantitatively measuring the diffusion within biological membranes in vivo is complicated and data evaluation is challenging. Thus, it is often desirable to study diffusion of specific molecules using in vitro model systems. Three model systems are commonly used: supported lipid bilayers (SLBs),[1] giant unilamellar vesicles (GUVs),[2] and black lipid membranes (BLMs).[3]

SLBs are artificial membranes attached to a solid support such as mica or glass. The lipids can either be bound directly to the surface via covalent or ionic bonds, or they can be attached to ultrathin polymer cushions on the substrate.[4] Commonly used methods for SLB formation are the Langmuir–Blodgett technique and vesicle spreading. On the one hand, the resulting samples are very stable against mechanical stress. On the other hand, SLBs have the disadvantage that only one side of the bilayer is accessible and, more severely, that the solid support influences the diffusion processes within the bilayer.[5] This makes SLBs unsuitable for deducing diffusion coefficients of free and undisturbed lipid membranes.

GUVs are vesicles with a diameter between 10–80 μm and can thus be considered as locally planar. They can be prepared by liposome electroformation[6,7] usually at low ionic strength, although GUV preparation at high ionic strength, that is, physiological conditions, has also been reported.[8] The resulting vesicles constitute solvent-free, free-standing bilayers. However, the solution inside the GUVs cannot be exchanged after formation. Since GUVs are very sensitive to osmotic pressure differences, changes in the ionic strength of the surrounding medium as compared to the inside of a GUV can lead to membrane fluctuations or even rupture.

BLMs are lipid bilayers spanned over a pore. They are prepared by dissolving lipids in an organic solvent and painting them over the pore. In this case, both sides of the bilayer are accessible. BLMs in large pores are rather stable and can be perfused from both sides individually. Moreover, their stability allows for keeping them at high ionic strengths in the surrounding medium and even at different ion concentrations on both sides of the bilayer.

Several techniques have been employed to investigate diffusion processes in membranes. Most of them are fluorescence-based methods. One example is single-particle tracking (SPT)[9] where fluorescently labeled molecules can be tracked by means of video microscopy. Alternatively, non-fluorescent tagging with colloidal gold or latex particles is possible. In fluorescence recovery after photobleaching (FRAP),[10] fluorescently labeled molecules are bleached irreversibly with a short laser pulse of high intensity. Fluorescent molecules then diffuse into the bleached region, thereby restoring the fluorescence signal. The signal is observed with a highly attenuated beam to avoid bleaching during recovery. Afterwards, the diffusion coefficient can be determined by analyzing the rate of fluorescence recov-

[a] K. Weiß, Prof. Dr. J. Enderlein
III. Institute of Physics
Georg-August-University Göttingen
Friedrich-Hund-Platz 1
37077 Göttingen (Germany)
E-mail: enderlein@physik3.gwdg.de
Homepage: http://www.joerg-enderlein.de

ery. FRAP, however, requires rather high concentrations of fluorescently labeled molecules. Another drawback of FRAP is that the data evaluation is far from trivial. In order to determine the diffusion coefficient, the focus diameter has to be precisely known which is difficult because it depends on manifold optical parameters.

Alternatively, fluorescence correlation spectroscopy (FCS)[11] can be used to measure diffusion in membranes.[12,13] In FCS, the fluorescence intensity fluctuations due to changing numbers of fluorescent molecules within a laser focus are monitored. The temporal dynamics of these intensity fluctuations are characterized by the diffusion of molecules into and out of the focus. The recorded signal is auto-correlated, and the obtained autocorrelation function (ACF) shows a temporal decay which is determined by the diffusion coefficient of the molecules. FCS requires only a low concentration of fluorescently labeled molecules within the detection volume and thus allows for working close to the infinite dilution limit. Due to the slow diffusion rates in membranes, however, longer measurement times are necessary to obtain a sufficient number of trajectories for accurate evaluation, and special care must be taken to avoid photobleaching of the sample. Moreover, accurate positioning of the focus on the bilayer is mandatory since any misplacement influences the results severely.

The original method to determine the correct focus position was to localize the point of maximum fluorescence intensity. However, it was shown by Benda et al.[14] that this does not necessarily coincide with the accurate focus position with respect to the bilayer. Instead, they employed so-called *z*-scan FCS, where the sample is scanned in 0.2 μm steps along the optical axis (*z*-axis) perpendicular to the bilayer plane. The particle number (PN) and the diffusion time τ_D are both dependent on the focus diameter (and thus on the intersection between diverging laser beam and membrane). With increasing vertical distance between laser beam waist and bilayer, the observed diffusion time increases. In the *z*-scan method, the observed dependence of diffusion time on vertical distance is fitted by a parabolic profile to determine the beam waist diameter and relative position between laser focus and membrane. This can then be used for calculating the lateral diffusion coefficient *D*. The disadvantage of this method is that it requires recording multiple ACFs at different vertical focus positions and is thus time-consuming and sensitive to mechanical drift of the setup.

Alternative approaches are line-scan FCS,[15] and dual-focus fluorescence correlation spectroscopy (2f-FCS).[16] In both methods, the core idea is to introduce an external length-scale into the measurement by placing two detection regions at a well-known distance from each other and to employ both, the ACFs from each region as well as the cross-correlation between them, for the analysis. In line-scan FCS, two parallel lines with known distance are scanned alternately. Cross-correlating both intensity traces yields a correlation curve which is characterized by the diffusion of the molecules from one detection volume to the other within the bilayer. Thus, the diffusion coefficient and the beam waist w_0 can be obtained directly by fitting the correlation curves without additional calibration measurements.[17] Moving the detection volume improves the statistical accuracy and decreases the measurement time as compared to stationary detection volumes. Moreover, the residence time of the molecules in the detection volume is decreased and the effect of photobleaching is minimized. Line-scan FCS is thus especially suitable for measurements of slow diffusion processes such as diffusion in membranes.

In 2f-FCS, two tightly overlapping foci are generated with the help of a birefringent crystal (Nomarski prism). The distance between the foci is precisely known and depends only on the optical properties of the Nomarski prism. Thus again, calibration with a known standard is unnecessary and the technique is robust against refractive index mismatch and optical saturation effects. In a recent publication,[18] 2f-FCS was used jointly with *z*-scan FCS combined to measure protein diffusion in GUVs, however without systematically studying the performance and accuracy of the method for membrane diffusion measurements.

Herein, we focus on the performance of 2f-FCS for precisely measuring diffusion coefficients within free-standing lipid model membranes (BLMs). The questions to be investigated are: How sensitive is 2f-FCS to the positioning of the laser beam waist with respect to the membrane, and correspondingly to membrane fluctuations? What is the influence of optical aberration caused by refractive index mismatch or coverglass thickness variation? Afterwards, we apply 2f-FCS for measuring lipid diffusion within BLMs as a function of ionic strength, ion valency, and lipid charge.

2. Theoretical Background

In this section, we present the theoretical background of 2f-FCS applied to diffusion measurements within a plane, and we investigate the impact of different optical aberrations on the performance and accuracy of the method.

A schematic of the setup is shown in Figure 1. The combined light of two laser beams with orthogonal polarization is sent through a Nomarski prism which deflects the orthogonally polarized light beams into slightly different angles, so that, after focusing through the objective, one generates two laterally shifted but overlapping foci. The fluorescence light which is generated in these foci is collected by the same objective (epi-fluorescence setup) and, after passing a dichroic mirror, focused through a circular aperture. The diameter of this aperture is large enough so that basically all light generated within the focal plane of the focused laser beams passes through. After the aperture, the light is refocused on sensitive single-photon detectors. In a 2f-FCS experiment, one determines the autocorrelation functions for each focus as well as the cross-correlation between foci. This can only be done if one has some means to distinguish which photon was generated within which focus. Experimentally, this is realized by alternate pulsing of both lasers, and by recording photon arrival times with picosecond temporal resolution. If the time interval between pulses is significantly larger than the typical fluorescence decay time of the used fluorescent dyes, one can unequivocally correlate each detected photon with the laser

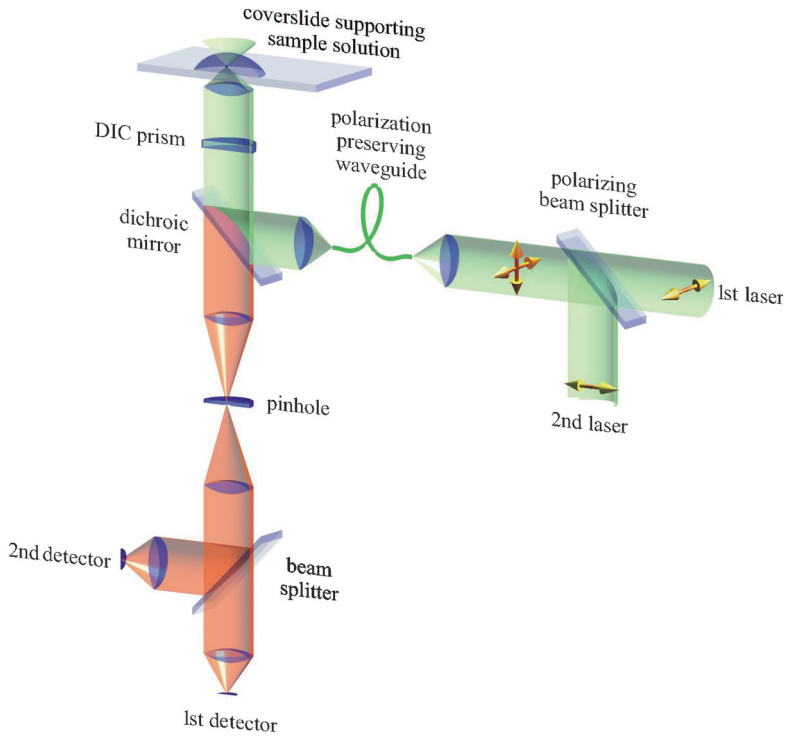

Figure 1. A 2f-FCS setup. The light of two perpendicularly polarized laser beams is combined by a polarizing beam splitter, sent through an optical fiber, and reflected towards the objective by a dichroic mirror. Before entering the objective, the light is passed through a Normarski prism which deflects the light depending on its polarization. After focusing the beams through the objective, two overlapping foci are generated. The resulting fluorescence light is then focused through a confocal aperture and detection is done with two detectors.

pulse that excited it, and thus with the focus where it was generated. Finally, by globally fitting the auto- and cross-correlation functions to a suitable model function, one can extract the diffusion coefficient of the diffusing molecules.

For modeling the performance of 2f-FCS in membrane diffusion measurements, we proceed in three steps. First, we calculate the molecule detection function (MDF) for both foci using an exact wave optical approach that takes also into account all polarization effects. Second, we use these calculated MDFs for modeling a 2f-FCS experiment on diffusing molecules confined to a single plane perpendicular to the optical axis. Last, we fit the calculated FCS curves with the fit model which is also used for experimental data analysis. By varying the modeled experimental conditions such as relative position of the molecule's plane with respect to the focus plane, solvent refractive index, or cover slide thickness, we check the impact of these different parameters on the fitted diffusion coefficient, and thus obtain a clear theoretical understanding of the expected performance of 2f-FCS measurements of membrane diffusion.

The MDF $U(\mathbf{r})$ describes the position-dependent joint probability to excite a fluorescent molecule at a given position and to detect a photon emitted from this position. Thus, the calculation of the MDF involves first the calculation of the light intensity distribution of the focused laser beam and second the calculation of the position-dependent efficiency of light detection by the confocal microscope. Both are done by using the classical approach of Richards and Wolf[19,20] for handling the transmission of light though optical systems with high numerical aperture. An extensive presentation and discussion of the technical details of these calculations for a 2f-FCS experiment can be found in ref. [21].

When denoting the MDF of the jth focus by $U_j(\mathbf{r})$, then the *lag-time dependent* part of the auto- and cross-correlation functions for a model 2f-FCS experiment on molecules diffusing within a plane situated at position z along the optical axis is given by Equation (1):

$$g_{jk}(t,z) = \frac{1}{4Dt}\int d\rho_2 \int d\rho_1 U_j(\rho_2,z) \exp\left[-\frac{|\rho_1-\rho_2-\delta_{jk}|^2}{4Dt}\right] U_j(\rho_1,z) \quad (1)$$

where $g_{jk}(t,z)$ is the correlation function of the fluorescence signal from focus j against that of focus k at lag time t, D denotes the diffusion coefficient, δ_{jk} accounts for the lateral distance between foci with $\delta_{jk}=0$ for $j=k$ and $\delta_{jk}=\delta$ for $j\neq k$ where δ is the non-zero focus distance vector. $\rho_{1,2}$ are radial position vectors perpendicular to the optical axis, and both integrations extend over the whole plane. When calculating these integrals numerically, the integration region is chosen large enough so that the MDFs decrease to negligible values.

Finally, the calculated correlation functions have to be fitted with a 2f-FCS fit model. For the diffusion within a plane, this fit model is quite simple: One assumes that the radial distribution of the MDFs within a plane at position z can be approximated by a two-dimensional Gaussian distribution function [Eq. (2)]:

$$U_j(\rho,z) \propto \exp\left(-\frac{2\rho^2}{w_j^2}\right) \quad (2)$$

where w_j defines the width of the of the Gaussian distribution for the jth focus. With this assumption, the correlation functions (up to some constant factor) are given by Equation (3):

$$\tilde{g}_{jk}(t,z) = \frac{1}{w_j^2+w_k^2+8Dt}\exp\left[-\frac{2\delta_{jk}^2}{w_j^2+w_k^2+8Dt}\right] \quad (3)$$

with both j and k being either equal to 1 or 2. $\tilde{g}_{jk}(t,z)$ now describe the model functions used for fitting experimental data, where $\tilde{g}_{11}(t,z)$ and $\tilde{g}_{22}(t,z)$ are the autocorrelation functions, and $\tilde{g}_{12}(t,z)$ and $\tilde{g}_{21}(t,z)$ are the cross-correlation functions. It should be noted that the exact dependence of the w_j on posi-

tion z is rather non-trivial, but when globally fitting the correlation curves, one treats both beam waist diameters w_1 and w_2 as fit parameters, together with the diffusion coefficient D.

2.1. Ideal Aberration-Free Optics

First, we want to check how well 2f-FCS performs when the plane of diffusing molecules is positioned at different values of z along the optical axis. In this section, all model calculations are performed for the following parameters: the numerical aperture of the objective is 1.2, and the objective is considered to be optically perfect when focusing/imaging in water (refractive index 1.33). The principal focal distance of the objective is assumed to be 3 mm, and the focal distance of the tube lens 180 mm, so that image magnification at the confocal aperture is 60×. The aperture diameter is set to 150 μm. The excitation wavelength is 640 nm, and the peak emission wavelength is 670 nm. All these values correspond to those of the experiments described below. It is furthermore assumed that the laser beam which is focused through the objective into the sample has a Gaussian intensity profile. For investigating how this focusing affects a 2f-FCS measurement, we have varied the $1/e^2$-radius of this Gaussian profile from 1.25 mm to 3.5 mm, thus covering the range from relaxed to nearly diffraction-limited focusing, as shown in Figure 2 by correlating the laser beam radius with the waist radius of the resulting focus in sample space.

Figure 3 presents the computational results for a 2f-FCS measurement on molecules diffusing within a plane under ideal optical conditions (no aberrations). Shown are the fitted values of the diffusion coefficients as a function of the position of the molecules' plane with respect to the focus' beam waist, and for different degrees of focusing. As can be seen, for laser-beam radius-values between 1.25 and ca. 2.25, one has a range of ca. plus/minus 0.5 μm around the focal plane where the average systematic error between fitted and actual value of the diffusion coefficient remains below 5%. For tighter focusing, this range narrows and one quickly obtains large systematic errors when the plane of the diffusing molecules moves farther away from the focal plane. The main reason for this is that with tighter focusing, the transversal excitation intensity profile can no longer be well approximated with a Gaussian distribution, which is, however, the basis of the correlation fit curves. Thus, when aiming at good accuracy and least sensitivity to focus placement, it is recommended to work with relaxed focusing, corresponding to focus beam waists of around 300 to 400 nm. The obtained results indicate also that 2f-FCS will be robust against vertical membrane fluctuations having amplitudes below a couple of hundred nanometers. This can be important when applying 2f-FCS to diffusion measurements in GUVs, where even slight differences in osmolarity between the in- and outside of the vesicle can cause non-negligible membrane fluctuations.

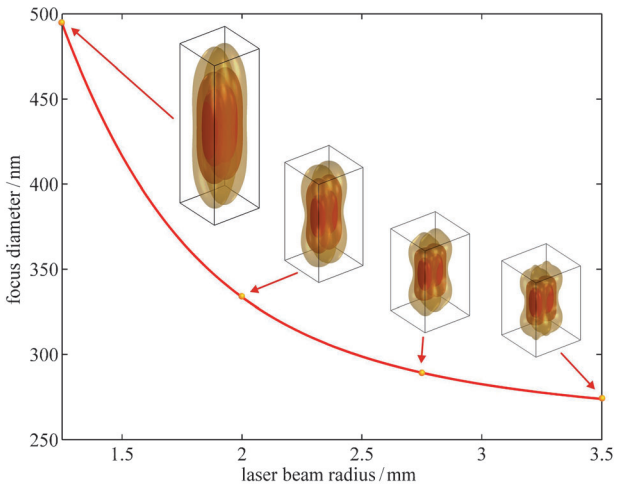

Figure 2. Radius of the laser beam that is coupled into the objective and the radius of the resulting focus in sample space. The insets show the shape of the two overlapping MDFs for selected laser beam radius values, each box has the same transversal size of 1.2 μm by 1.6 μm. Shown are the iso-surfaces, for both foci, where the combined excitation and detection efficiency for a fluorescence photon has fallen off to $1/e^2 \sim 13\%$ of its maximum value in the very center of the focus.

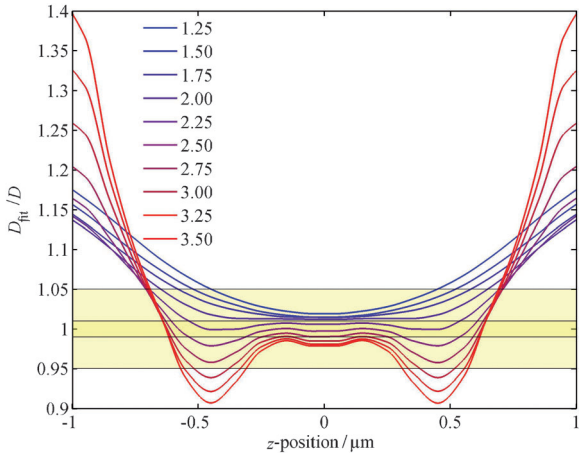

Figure 3. Modeling a 2f-FCS measurement of molecular diffusion within a plane under ideal optical conditions (no aberrations). Shown is the ratio of fitted values to actual values of the diffusion coefficients as a function of the position of the plane with respect to the beam waist, and for different degrees of focusing. Here and in the following figures, the legend indicates the radius values of laser beam coupled into the objective in mm. Shaded areas indicate 1% and 5% error margins.

2.2. Aberration by Refractive Index Mismatch and Cover-Slide Thickness Deviation

Two of the most common and nearly unavoidable origins of optical aberrations in FCS experiments are deviation of the cover slide thickness from its design value to which the objective is adjusted, and refractive index mismatch between sample solution and the objective's immersion medium. When working with free-standing lipid membranes, either GUVs or BLMs, the distance between membrane and cover slide surface is typically rather large (on the order of 100 μm). Thus, even slight mismatches in refractive indices accumulate over the long optical path length and cause large aberrations. First, we

consider the situation of refractive index mismatch. As a typical example, we assume that the sample solution has a refractive index of 1.36 instead of 1.33 for pure water, and that the focal plane of the objective is located 100 μm above the cover slide. For this situation, the top panel of Figure 4 depicts the computational result of the model 2f-FCS measurements, again showing the fitted diffusion coefficient as a function of the *z*-position along the optical axis (position of the bilayer, that is, the plane of diffusing molecules). The graphs purposefully start at a *z*-position larger than 100 μm because positioning the foci 100 μm above the cover slide by moving the objective by that distance in a real experiment actually places the focus deeper in solution due to refractive index mismatch. Here and hereafter, we restrict ourselves to considering only the cases of relaxed focusing (laser beam radius below 2 mm).

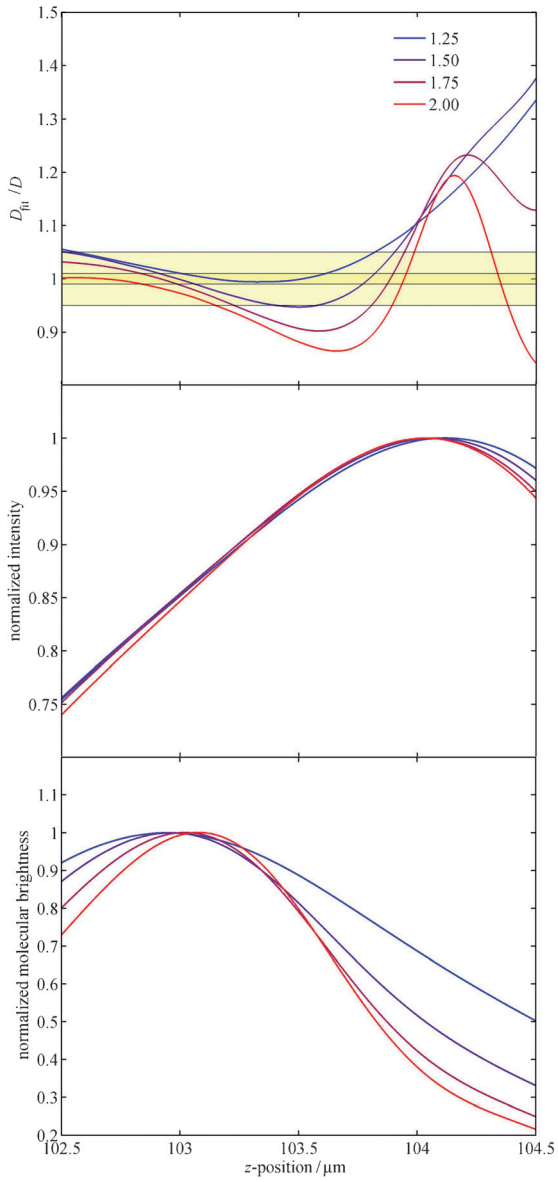

Figure 4. Modeling a 2f-FCS measurement with aberrations caused by refractive index mismatch. Top panel: Fitted diffusion coefficient relative to its exact value. Shaded areas indicate 1% and 5% error margins. Middle panel: Mean fluorescence intensity (average over plane). Bottom panel: Molecular brightness. All curves given as a function of position along the optical axis.

In a real experiment, one still has to find the correct position of the laser focus with respect to the membrane. One option would be to adjust the focal plane to the maximum of fluorescence intensity. The middle panel in Figure 4 shows the fluorescence intensity (integrated over the whole plane of the membrane) as a function of focus position. As can be seen, the position of maximum intensity is shifted to larger *z*-values compared to the region of least systematic error of the 2f-FCS measurement given in Figure 4 (top panel). Thus, choosing the position of maximum intensity for measurement would result in a systematic overestimation of the diffusion coefficient. The reason for this shift is the not so widely recognized fact that spherical aberrations always place the maximum of the detection efficiency distribution at a different position along the optical axis than the minimum beam waist of the focused laser beam. This has the effect that the transversal profile of the MDF becomes quickly non-Gaussian when moving away from the plane of tightest focus diameter. This is not a specific problem of 2f-FCS, but will also affect line-scan or scanning focus FCS. The only FCS method which does not suffer from this problem is z-scan FCS, but for the price of ca. 10 times longer measurement times for the whole z-stack of FCS measurements. Another option is to search for the position of maximum molecular brightness. For a fixed molecular concentration (molecules per unit area), the mean number of molecules within the detection area is proportional to that area which is given by Equation (4)

$$V_{\mathrm{eff}}(z) = \left[\int d\rho U(\rho, z)\right]^2 / \int d\rho U^2(\rho, z) \tag{4}$$

Furthermore, the mean observable fluorescence intensity from one molecule is proportional to [Eq. (5)]:

$$\bar{I}(z) = \int d\rho U(\rho, z) \tag{5}$$

Thus, the average observable molecular brightness for molecules diffusing within a plane at position z will be proportional to $\bar{I}(z)/V_{\mathrm{eff}}(z)$. The calculated (normalized) brightness values as a function of position *z* are shown in Figure 4 (lower panel). As can be seen, the position of maximum molecular brightness is a much better choice for obtaining correct diffusion coefficients from a 2f-FCS measurement. Thus, in the experiments described below, we have followed this procedure for finding the correct position of focus with respect to the lipid membrane.

A second important origin of aberration is cover slide thickness deviations. State-of-the-art water immersion objectives are designed to take into account the presence of a glass cover slide of specific thickness between the objective and the sample. Most of these objectives also have adjustment rings for matching them to a specific cover slide thickness. In practice, however, cover slides rarely have the exact thickness value as indicated by the supplier, and correct positioning of an objective's adjustment ring is far from trivial. Thus, devia-

tions of the order of 10 μm between the actual cover slide thickness and the value an objective is adjusted to are mostly unavoidable. Although this is close to undetectable in typical imaging applications of a microscope, FCS experiments are extremely sensitive to size and shape changes of the MDF. As an example, we consider here a cover slide thickness deviation of only 10 μm. The top panel of Figure 5 again shows the values

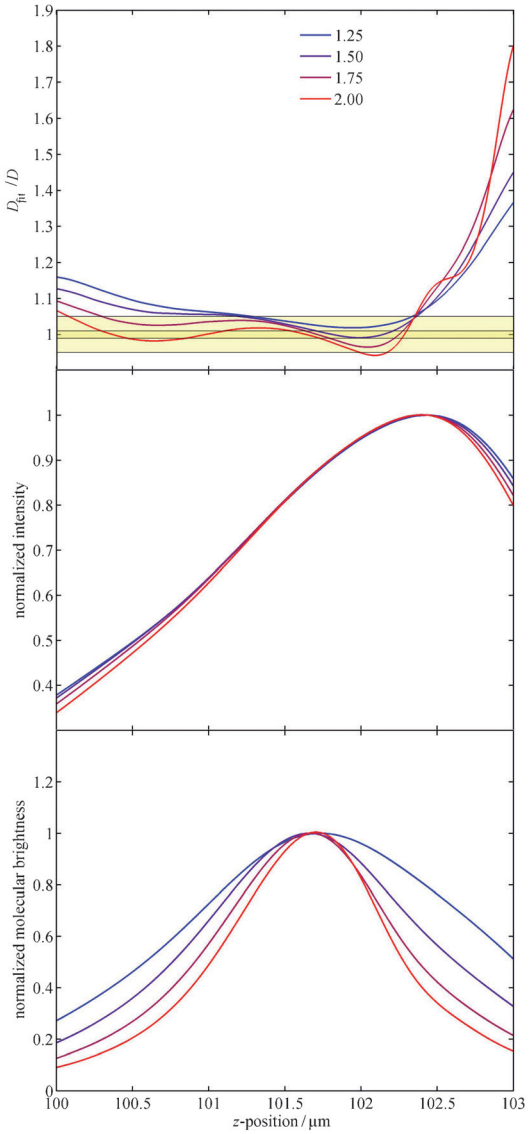

Figure 5. Modeling a 2f-FCS measurement with aberrations caused by cover slide thickness deviation. Top panel: Fitted diffusion coefficient relative to its exact value. Shaded areas indicate 1% and 5% error margins. Middle panel: Mean fluorescence intensity (average over plane). Bottom panel: Molecular brightness. All curves given as a function of position along the optical axis.

of fitted diffusion coefficients as a function of focal plane position, and the middle and lower panel of the same Figure depict the corresponding profile of the fluorescence intensity and molecular brightness, respectively. Again, we see a shift between the position of maximum intensity and the region of least systematic error, although not as dramatic as caused by the refractive index mismatch. And again, the position of maximum molecular brightness is a better choice for minimizing systematic errors in diffusion coefficient determination.

Experimental Section

BLM Formation

Neutral BLMs were formed from a mixture of 40 weight percent 1-palmitoyl-2-oleoyl-sn-glycero-3-phosphocholine (POPC, Avanti Polar Lipids, Alabaster, USA) and 60 weight percent 1-palmitoyl-2-oleoyl-sn-glycero-3-phosphoethanolamine (POPE, Avanti Polar Lipids, Alabaster, USA) in dodecane which ensured a homogeneous mixture of the two lipids and a bilayer in the liquid disordered phase.[22] For generating negatively charged BLMs, the previously described lipid mixture of POPC and POPE was mixed with 1 weight% 1,2-di-(9Z-octadecenoyl)-*sn*-glycero-3-phospho-(1′-*rac*-glycerol) (DOPG, Avanti Polar Lipids, Alabaster USA). The lipid solutions were prepared by mixing appropriate amounts of POPC and POPE or POPC, POPE and DOPG, respectively, in chloroform. Afterwards, chloroform was evaporated for 20 min in high vacuum and dodecane was added to the dry lipid mixture. Then, Atto655-labeled 1,2-dihexadecanoyl-sn-glycero-3-phosphoethanolamine ($DPPE^{Atto655}$) dissolved in chloroform was added in a molar ratio of 1:4000000. The concentration of the fluorescent lipid solution was chosen so that 0.08 μL of chloroform solution were added to 30 μL of lipid solution in dodecane. Thus, the effect of chloroform is negligible. Preparing the lipid mixtures may introduce an error due to slight differences in pipetted lipid amounts. This error, however, seems to be very small and within the 5% error of the measurement, since no influence on the obtained diffusion coefficients was observed for different lipid samples of the same kind under the same conditions.

Herein, the Ionovation Bilayer Explorer is used to generate BLMs. Its main part is the Bilayer Slide (Figure 6) which is connected to a HEKA EPC 10 Patch Clamp amplifier. The Bilayer Slide consists of a

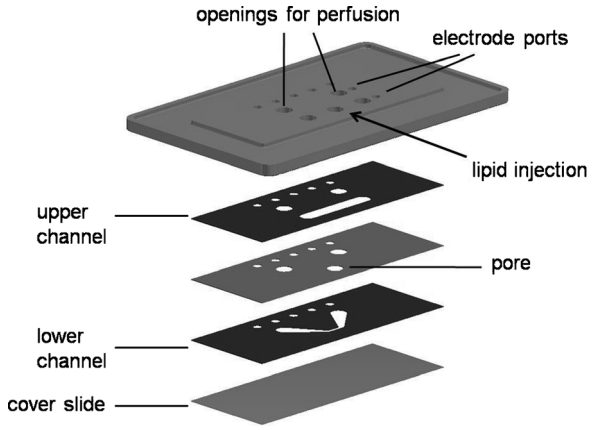

Figure 6. Bilayer slide with a pore diameter of 120 μm for BLM synthesis.

cover slide on the bottom and a teflon pore of 120 μm diameter which is surrounded by an upper and a lower perfusion channel. On the top, the slide contains openings for perfusion and lipid injection as well as two electrode ports. The latter reach into the upper and lower perfusion channel, respectively, and are connected to the patch clamp amplifier.

Table 1. Used lipid and buffer compositions.

Lipid mixture	Ion concentration varied	Buffer
POPC/POPE	Ca^{2+}	50 mM TRIS, 150 mM NaCl, 5 mM KCl
POPC/POPE	K^+	50 mM TRIS, 150 mM NaCl, 5 mM KCl
POPC/POPE	Na^+	50 mM TRIS (except at first point: 50 mM TRIS, 5 mM KCl)
POPC/POPE/DOPG	Ca^{2+}	50 mM TRIS, 150 mM NaCl, 5 mM KCl
POPC/POPE/DOPG	K^+	50 mM TRIS
POPC/POPE/DOPG	Na^+	50 mM TRIS

In order to generate BLMs, 0.2 μL of the lipid mixture in dodecane were added to the Bilayer Slide which itself contained an aqueous buffer (see Table 1). The lipids were painted over the pore employing an automated pumping cycle. Bilayer formation was monitored via capacitance measurements.

Our setup allows perfusion of both sides of the bilayer individually and thus varying the ionic strength on either one or both sides of the BLM. Moreover, the BLM is accessible with a high numerical aperture (N.A.) objective and 2f-FCS diffusion measurements can be conducted.

Finally, for all the buffers used in our experiments, the refractive index was measured to be 1.34, slightly larger than that of pure water which was 1.33. The refractive indices were determined with a refractometer (Carl Zeiss, Germany) at room temperature. The buffers of different ionic strength were all prepared by diluting a stock solution of higher concentration to minimize errors especially in the calcium concentration series. Some concentrations of this series (5 mm, 6 mm, 8 mm CaCl2) were even measured with buffers made from two different stock solutions to determine the error. The same diffusion coefficients were obtained in 2f-FCS with both solutions indicating that the error is within 5%.

Dual-Focus Fluorescence Correlation Spectroscopy

The principal measurement setup used for the experimental work is described in Figure 1. It is a commercial confocal microscopy system (MicroTime 200 with dual-focus option, PicoQuant GmbH, Berlin, Germany) which is similar to the setup described in detail in ref. [16] In summary, the light of two identical, linearly polarized pulsed diode lasers (wavelength 640 nm, pulse duration 50 ps fwhm) is combined by a polarizing beam splitter. Both lasers are pulsed alternately with a repetition rate of 40 MHz (pulsed interleaved excitation or PIE).[23] The cw-power of the lasers had been adjusted to 3 μW each. Both beams are coupled into a polarization-maintaining single mode fiber. At the fiber output, the light is collimated and reflected by a dichroic mirror (FITC/TRITC Chroma Technology, Rockingham, VT, USA) towards the microscope's objective (UPLSAPO 60×W, 1.2 N.A., Olympus Deutschland GmbH, Hamburg, Germany). Before entering the objective, the light is passed through a Nomarski prism deflecting the light from both laser diodes into slightly different directions, so that after focusing one obtains two laterally shifted but overlapping excitation foci with 450 nm distance. The exact interfocal distance was determined by performing 2f-FCS on a solution of fluorescent polymer beads of known radius, for details see ref. [24] Although three-dimensional diffusion processes are used for calibration, the obtained foci distance from the respective fits corresponds to the actual distance between the foci (as was shown in ref. [25] and is also verified by the theoretical calculations in the present paper) and will be also valid in two dimensions.

Fluorescence is collected by the same objective, passed through the dichroic mirror, and focused onto a single circular aperture (diameter 150 μm). Using a pinhole is optional for diffusion measurements in membranes. However, due to the restriction in the *z*-direction, only fluorescence from the membrane and not from the surrounding solution is collected. As a consequence, a measurement is less sensitive to impurities in the surrounding buffer. This is not so essential in case of lipid diffusion measurements, since the fluorescently labeled molecules are added directly to the lipid solution. The chances of (hydrophobic) fluorescently labeled molecules entering the (hydrophilic) environment around the BLM are rather small. For measurements involving proteins which are added to the buffer solution and possibly contain free dye, using a pinhole is much more required since it yields better signal-to-noise ratio, which is essential for FCS measurements.

After the pinhole, the light is collimated, split by a 50/50 beam splitter, and focused onto two single-photon avalanche diodes (APDs, two SPCM-AQR-13, PerkinElmer Optoelectronics, Wiesbaden, Germany). Single-photon counting electronics (HydraHarp 400, PicoQuant GmbH, Berlin, Germany) record the detected photons of both detectors independently with an absolute temporal resolution of two picoseconds on a common time frame.

As already mentioned in the Section 2, recording photon detection times with picosecond resolution allows for associating each fluorescence photon with the laser pulse that has excited it, and thus with the focus it was excited in. With this information, the auto- and cross-correlation curves are calculated using a dedicated software algorithm.[21] To avoid any impact from afterpulsing of the APDs[26] on the finally computed correlation curves, one correlates only photon pairs that have been detected by both detectors. In total, one calculates four autocorrelation curves (for example correlating photons excited by laser 1 and detected by detector 1 against photons excited by laser 1 and detected by detector 2, and so on), and six cross-correlation functions (for example correlating photons excited by laser 1 and detected by detector 2 against photons excited by laser 2 and detected by detector 1, and so on), taking into account also the temporal order of the correlated photon pairs (i.e. whether the first photon was excited by the first laser and the second by the second or vice versa).

Finally, fitting of the data is done with the model curves presented in the Theory section, assuming Gaussian shapes of the cross sections of the MDFs with the membrane. Thus, one finally has three crucial fit parameters: the two diameters of the Gaussian profiles, and the diffusion coefficient.

3. Results

3.1. Dual-Focus Fluorescence Correlation Spectroscopy in BLMs

For adjusting the focus position on the BLM, images of the pore and the bilayer are taken prior to each measurement (Figure 7). Then, the focus is placed at the observed position of maximum intensity. As was mentioned in the theory section, this does not necessarily lead to the optimal position yielding minimum error. Thus, short FCS measurements around the position of maximum intensity are performed to find the position

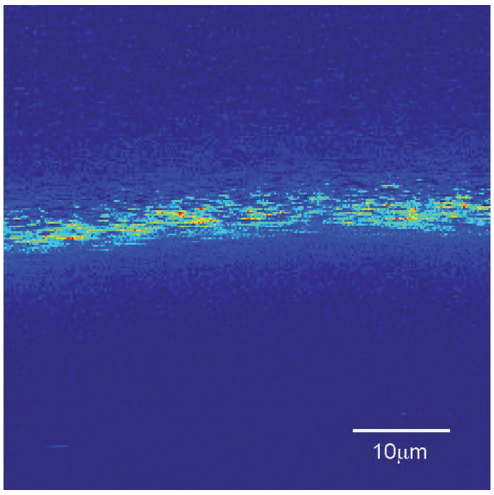

Figure 7. *z*-Scan of a POPC/POPE bilayer with head-group labeled DPPE^{Atto655}. Shown is the convolution of the bilayer image with its point spread function which makes it appear broader than the actual BLM.

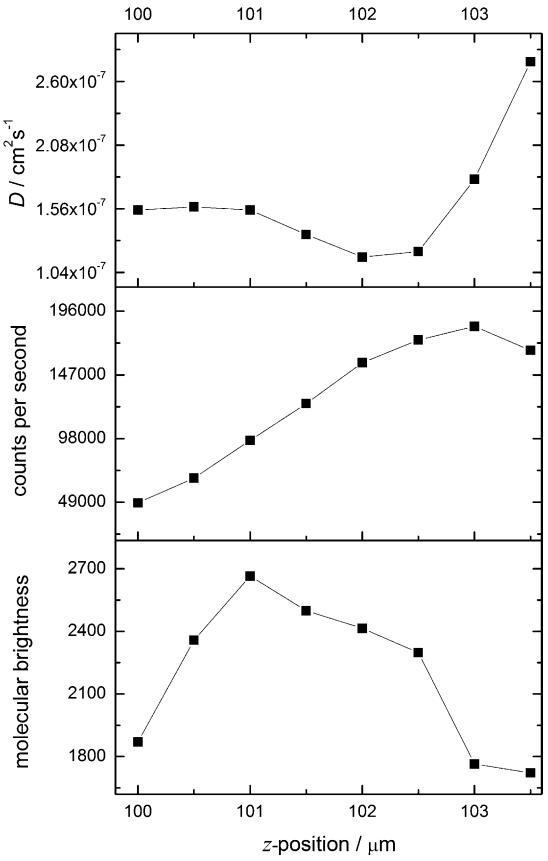

Figure 8. Scan of a 2f-FCS measurement across a BLM. Shown are the obtained diffusion coefficients (top), the count rate (i.e. mean intensity) (middle) and the count rate per molecule (i.e. molecular brightness) (bottom) as a function of focus position.

of maximum molecular brightness, which is then used for the diffusion measurements.

In general, when performing FCS measurements on membranes, one concern is that the bilayer may move out of focus during the measurement (mechanical drift). This is avoided by choosing short measurement times of 10 min and by re-adjusting the foci before each measurement. Moreover, bilayer movement out of focus and rupture of the bilayer during the measurement lead to a pronounced decrease in the count rate and loss of correlation. Therefore, meaningful correlation curves with an intact bilayer and correct bilayer position can be distinguished from flawed ones. All measurements are performed at laser powers of 3 μW to avoid photobleaching. The count rate remained constant during the measurements, except when the bilayer moved out of focus or ruptured during the measurement which confirms that photobleaching was not a problem.

For checking the presence of aberrations in our experiments, we performed 2f-FCS measurements at different positions across a BLM (*z*-Scan). The result for the diffusion coefficients is shown in Figure 8 (top panel), the corresponding intensity values can be found in the middle panel, and the molecular brightness (counts per second per molecule) in the lower panel of Figure 8. Since many different positions had to be measured during the *z*-Scan, the measurement time was limited to only 200 seconds to avoid mechanical drift of the setup and to decrease the chance of bilayer movement or rupture during the experiment. The obtained curves for the diffusion coefficients and intensities are in good qualitative agreement with the modeled curves in Figure 5, showing the effects of aberrations caused by refractive index mismatch and cover slide thickness deviation. Most striking is the drastic increase in obtained diffusion coefficients between *z*-positions 102.5 μm and 103 μm which is also confirmed by the theoretical calculations. The reason for this increase is that the intensity profile of the laser beams cannot be approximated by a Gaussian profile anymore as soon as the membrane is not longer at the position of maximum focusing, that is, the plane of maximum molecular brightness. The data evaluation, however, is based on the assumption of a Gaussian profile of the laser beams. If this assumption becomes invalid, the resulting fits for the auto- and crosscorrelation curves worsen significantly and the obtained diffusion coefficients deviate strongly from its actual value.

In summary, 2f-FCS provides a robust tool to study membrane diffusion. To find the correct focus position on the BLM, the membrane was placed in the plane of maximum molecular brightness, which has proven to give reliable results in the theoretical calculations. This procedure, however, would not work with single focus FCS, since there even the focus diameter in the plane of maximum brightness can change from measurement to measurement due to all kinds of possible aberrations. The only method with comparable performance as 2fFCS is z-Scan FCS. The significant drawback of this method, however, is that it is very time-consuming which is problematic, especially in rather instable systems where short measurement times are required.

3.2. Measurements of Lipid Diffusion in BLMs

In order to test the effect of mono- and divalent ions on lipid diffusion in neutral and negatively charged BLMs, we investigated diffusion coefficients of $DPPE^{Atto655}$ in POPC/POPE (neutral) and POPC/POPE/DOPG (negatively charged) bilayers with 1 weight% DOPG. The different lipid and buffer compositions used are listed in Table 1. For the FCS measurements, headgroup labeled lipids were chosen to avoid any effect of the fluorescent dye on the phase behavior of the lipids. Moreover, only small concentrations (much less than 1 molecule per μm^2) of Atto655-labeled 1,2-dihexadecanoyl-sn-glycero-3-phosphoethanolamine ($DPPE^{Atto655}$) are required for 2f-FCS measurements. In our study, adding the labeled lipids in a (molar) ratio of 1: 4000000 with respect to POPE was found to be sufficient. Slightly larger concentrations of labeled lipids may decrease the amplitude of the correlation curves but do not affect the obtained diffusion coefficient.

The resulting auto- and cross-correlation curves (Figure 9) could be fitted well with the two-dimensional model described above. BLMs were generated in buffers with different ionic strength varying the calcium, sodium or potassium ion concentration individually. Whether the bilayers were newly formed in the respective buffer or an already existing bilayer was perfused with a buffer of different ionic strength did not make a difference. In the latter case, special care was taken to perfuse the BLMs with a sufficient amount of buffer and thus to ensure complete buffer exchange. Also, we allowed for an equilibration time of 10 min in this case.

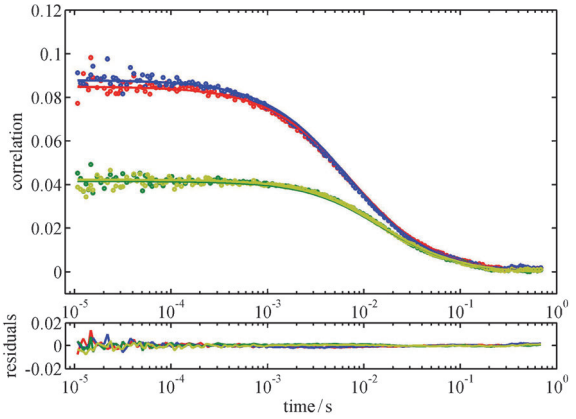

Figure 9. Curves for lipid diffusion within a POPC/POPE bilayer with headgroup labeled $DPPE^{Atto655}$ in 50 mM TRIS (pH 7.5) with 150 mM NaCl, 5 mM KCl and 3 mM $CaCl_2$. The lipid mixture contained 6 mg mL^{-1} POPE, 4 mg mL^{-1} POPC and 3.3×10^{-6} mg mL^{-1} $DPPE^{Atto655}$. The red and blue curves are the autocorrelations of each focus, and the green and yellow curves are the cross-correlations between both foci (first focus against second, and vice versa). Solid lines are fits to the data (circles).

Each measurement was performed at least three times for 10 min. All collected photons were divided into bunches of 10^6 photons per bunch. One measurement yielded on average 60 bunches. If less bunches were created during one measurement (i.e. due to bilayer rupture), the measurements were repeated up to five times to generate a similar amount of bunches and ensure statistical accuracy. This was especially necessary at low ionic strength because the BLMs were relatively unstable under these conditions. All determined diffusion coefficients are presented in Figure 10. The respective standard deviation was 5% or less, except for measurements at very low ionic strength. The error increases in this case due to instability of the bilayer.

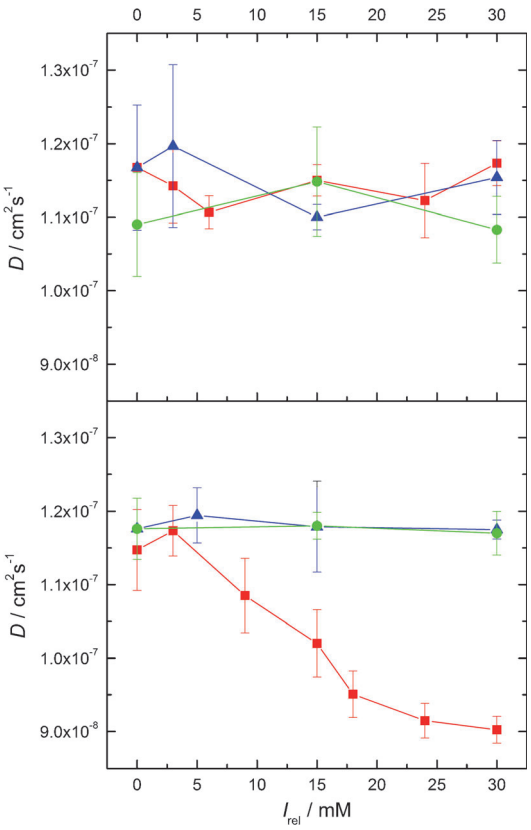

Figure 10. Influence of mono- and divalent cations on lipid diffusion in neutral (top) and charged BLMs (bottom). Red curves: variation of $c(CaCl_2)$, blue curves: variation of c(KCl), green curves: variation of c(NaCl). The buffers used are listed in Table 1. Top panel: in neutral POPC/POPE bilayers, no electrostatic interaction is observed. The lipid diffusion coefficient remains constant upon varying the ionic strength. Bottom panel: diffusion in negatively charged bilayers of POPC/POPE with 1 weight% DOPG is not influenced upon addition of monovalent ions. Addition of divalent ions, however, significantly decreases the diffusion coefficient. Standard deviation for the measurements is 5% or less, except for measurements at low ionic strength where the errors increase due to instability of the BLM.

Generally, variation of the ion concentration in neutral lipid bilayers did not lead to a systematic change in the lipid's diffusion coefficient. Neither calcium nor potassium or sodium ions did have an effect on lipid diffusion in a POPC/POPE BLM. Fluctuations in the obtained diffusion coefficients were found especially at very low ionic strengths since neutral BLMs are harder to form and less stable as mentioned above. Charged BLMs, however, are more stable at low ionic strength compared to the neutral POPC/POPE bilayers and were thus less prone to fluctuations.

For negatively charged POPC/POPE/DOPG bilayers, the diffusion coefficients remained constant when increasing sodium or

potassium ion concentration up to 30 mM (green and blue curves in the lower panel of Figure 10). Comparing these values with the first point of the red curve in the lower panel of Figure 10, where the lipid diffusion was measured in 50 mM TRIS with 5 mM KCl and 150 mM NaCl (see Table 1), we can state that the diffusion coefficient remains constant even upon increase of the sodium concentration up to 150 mM. Thus, we can conclude that monovalent ions also do not influence lipid diffusion in charged BLMs for our system.

This is in strong contrast to the results reported in ref. [27] where the authors used conventional single-focus FCS as well as molecular dynamics simulations for determining diffusion coefficients. They report a rather drastic decrease in the lipids' diffusion coefficients to about half of the original value in a neutral POPC SLB upon addition of 100 mM NaCl with charged and uncharged dyes. A decrease in diffusion coefficients was also found by Hof et al.,[28] who measured lipid diffusion in DOPC SLBs, also using single-focus FCS. The observed decrease in diffusion coefficients is about 20%. Both studies use SLBs which might be problematic since the support can influence the diffusion processes. Since the influence of NaCl in ref. [28] is significantly less pronounced than in ref. [27] despite using a similar system, the drastic influence of sodium ions on lipid diffusion must be questioned. Furthermore, compared to our measurements, the obtained diffusion coefficients in ref. [28] have a much larger standard deviation of up to 16% and only two concentrations (0 mM and 150 mM NaCl) were investigated. Taking this into account, the influence of sodium ions might also be insignificant in their system and thus agree with our data. Also, our results are in good agreement with ref. [29] where the authors used pulsed field-gradient NMR for diffusion measurements in lipid membranes and also find no influence of monovalent ions on the lipid diffusion.

Upon addition of calcium, lipid diffusion in the negatively charged BLMs was slowed down significantly. This effect becomes prominent after addition of 3 mM $CaCl_2$ to the buffer. Since physiological calcium concentrations are usually in the nanomolar or, for certain cellular functions, locally in the micromolar range, the concentrations investigated are well above the calcium concentration in cells. The physiological range, however, is fully covered within the data since buffer solutions without and with 1 mM $CaCl_2$ can be compared. As can be seen, lipid diffusion in our system is not influenced by calcium ions under physiological conditions. A significant decrease in diffusion coefficients is only observed at an approximately 10^4 times higher calcium concentration.

The reason for the decrease in diffusion coefficient is electrostatic interaction between the divalent ions and the negatively charged lipid head groups. Calcium can bridge the negatively charged lipids together thus increasing the viscosity in the BLM. As a result, the lipid diffusion is slowed down. Monovalent ions, such as sodium and potassium, do not have a significant effect in our system. While they might be able to penetrate into the head group region of the bilayer, they do not seem to bridge neighboring lipids to such an extent (if any) that lipid diffusion is slowed down.

4. Conclusions

We combined 2fFCS with BLM systems which yields an accurate and robust technique for diffusion measurements in lipid bilayers. Correct positioning of the foci on the BLM is mandatory and achieved by choosing the position of maximum molecular brightness prior to the measurement. In our setup, both sides of the BLM are accessible and can be perfused individually which allows free adjustment of ionic strength and buffer composition on both sides of the membrane. Moreover, the BLM stability allows bilayer formation at high ionic strength. We used 2f-FCS to systematically study lipid diffusion in BLMs as a function of ion valency and concentration in the surrounding buffer. It was found that monovalent ions do not influence lipid diffusion, neither within uncharged nor in charged lipid membranes. However, divalent Ca^{2+} ions did slow down lipid diffusion within charged membranes at high ionic strength, indicating cross-bridging of lipids by calcium ions, thus increasing membrane viscosity.

Acknowledgement

We thank Christian Eggeling (MPI Biophysical Chemistry, Göttingen) for providing us with fluorescently labeled (Atto655) lipid, and Christoph Pieper and Ingo Gregor for their continuous technical support. Financial support by the Deutsche Forschungsgemeinschaft (project A 10, SFB 803) is gratefully acknowledged.

Keywords: fluorescence · fluorescence correlation spectroscopy · lipids · membrane diffusion · membranes

[1] A. A. Brian, H. M. McConnell, *Proc. Natl. Acad. Sci. USA* **1984**, *81*, 6159–6153.
[2] Y. Gambin, M. Reffay, E. Sierecki, F. Homblé, R. S. Hodges, N. S. Gov, N. Taulier, W. Urbach, *J. Phys. Chem. B* **2010**, *114*, 3559–3566.
[3] M. Winterhalter, *Curr. Opin. Colloid Interface Sci.* **2000**, *5*, 250–255.
[4] E. Sackmann, *Science* **1996**, *271*, 43–48.
[5] T. Dertinger, I. von der Hocht, A. Benda, M. Hof, J. Enderlein, *Langmuir* **2006**, *22*, 9339–9344.
[6] M. I. Angelova, D. S. Dimitrov, *Faraday Discuss.* **1986**, *81*, 303–311.
[7] M. Przybylo, J. Sýkora, J. Humpolíckova, A. Benda, A. Zan, M. Hof, *Langmuir* **2006**, *22*, 9096–9099.
[8] L.-R. Montes, A. Alonso, F. M. Goñi, L. A. Bagatolli, *Biophys. J.* **2007**, *93*, 3548–3554.
[9] *Single Particle Tracking and Single Molecule Energy Transfer* (Eds.: C. Bräuchle, D. C. Lamb, J. Michaelis), Wiley-VCH, Weinheim, **2009**.
[10] D. Axelrod, D. Koppel, J. Schlessinger, E. Elson, W. W. Webb, *Biophys. J.* **1976**, *16*, 1055–1069.
[11] R. Rigler, E. L. Elson, *Fluorescence Correlation Spectroscopy*, Springer, Berlin, **2001**.
[12] N. Kahya, P. Schwille, *Mol. Membr. Biol.* **2006**, *23*, 29–39.
[13] I. R. Bates, P. W. Wiseman, J. W. Hanrahan, *Biochem. Cell Biol.* **2006**, *84*, 825–831.
[14] A. Benda, M. BeneŠ, V. Mareček, A. Lhotský, W. T. Hermens, M. Hof, *Langmuir* **2003**, *19*, 4120–4126.
[15] J. Ries, S. Chiantia, P. Schwille, *Biophys. J.* **2009**, *96*, 1999–2008.
[16] T. Dertinger, V. Pacheco, I. von der Hocht, R. Hartmann, I. Gregor, J. Enderlein, *ChemPhysChem* **2007**, *8*, 433–443.
[17] J. Ries, P. Schwille, *Phys. Chem. Chem. Phys.* **2008**, *10*, 3487–3497.
[18] J. Kriegsmann, I. Gregor, I. von der Hocht, J. Klare, M. Engelhard, J. Enderlein, J. Fitter, *ChemBioChem* **2009**, *10*, 1823–1829.
[19] E. Wolf, *Proc. R. Soc. London Ser. A* **1959**, *253*, 349–357.

[20] B. Richards, E. Wolf, *Proc. R. Soc. London Ser. A* **1959**, *253*, 358 – 379.
[21] M. Wahl, I. Gregor, M. Patting, J. Enderlein, *Opt. Express* **2003**, *11*, 3583 – 3591.
[22] B. Cannon, M. Hermansson, S. Györke, P. Somerharju, J. A. Virtanen, K. H. Cheng, *Biophys. J.* **2003**, *85*, 933 – 942.
[23] B. K. Müller, E. Zakychikov, C. Bräuchle, D. C. Lamb, *Biophys. J.* **2005**, *89*, 3508 – 3522.
[24] C. B. Müller, K. Weiß, W. Richtering, A. Loman, J. Enderlein, *Opt. Express* **2008**, *16*, 4322 – 4329.
[25] T. Dertinger, A. Loman, B. Ewers, C. B. Müller, B. Krämer, J. Enderlein, *Opt. Express* **2008**, *16*, 14353 – 14368.
[26] M. Höbel, J. Ricka, *Rev. Sci. Instrum.* **1994**, *65*, 2326 – 2336.
[27] R. A. Böckmann, A. Hac, T. Heimburg, H. Grubmüller, *Biophys. J.* **2003**, *85*, 1647 – 1655.
[28] R. Vácha, S. W. I. Siu, M. Petrov, R. A. Böckmann, J. Barucha-Kraszewska, P. Jurkiewicz, M. Hof, M. L. Berkowitz, P. Jungwirth, *J. Phys. Chem. A* **2009**, *113*, 7235 – 7243.
[29] A. Filippov, G. Orädd, G. Lindbolm, *Chem. Phys. Lipids* **2009**, *159*, 81 – 87.

Received: September 5, 2011
Revised: December 15, 2011
Published online on January 17, 2012

